SPIE Defense and Security Symposium, Orlando, Florida USA, 17 – 21 April 2006
Non-Intrusive Inspection Technologies

Detection of nuclear material by photon activation inside cargo containers

Mehdi Gmar[*a], Eric Berthoumieux [b], Sébastien Boyer [b], Frédérick Carrel [a], Diane Doré[b], Marie-Laure Giacri [b], Frédéric Lainé [a], Bénédicte Poumarède[a], Danas Ridikas[b], Aymeric Van Lauwe[b]
[a]CEA Saclay, DRT/LIST/DETECS/SSTM, 91191 Gif-sur-Yvette, France
[b]CEA Saclay, DSM/DAPNIA/SPhN, 91191 Gif-sur-Yvette, France

ABSTRACT

Photons with energies above 6 MeV can be used to detect small amounts of nuclear material inside large cargo containers. The method consists in using an intense beam of high-energy photons (bremsstrahlung radiation) in order to induce reactions of photofission on actinides. The measurement of delayed neutrons and delayed gammas emitted by fission products brings specific information on localization and quantification of the nuclear material. A simultaneous measurement of both of these delayed signals can overcome some important limitations due to matrix effects like heavy shielding and/or the presence of light elements as hydrogen. We have a long experience in the field of nuclear waste package characterization by photon interrogation and we have demonstrated that presently the detection limit can be less than one gram of actinide per ton of package. Recently we tried to extend our knowledge to assess the performance of this method for the detection of special nuclear materials in sea and air freights. This paper presents our first results based on experimental measurements carried out in the SAPHIR facility, which houses a linear electron accelerator with the energy range from 15 MeV to 30 MeV. Our experiments were also modeled using the full scale Monte Carlo techniques. In addition, and in a more general frame, due to the lack of consistent data on photonuclear reactions, we have been working on the development of a new photonuclear activation file (PAF), which includes cross sections for more than 600 isotopes including photofission fragment distributions and delayed neutron tables for actinides. Therefore, this work includes also some experimental results obtained at the ELSA electron accelerator, which is more adapted for precise basic nuclear data measurements.

keywords: photofission, delayed neutron, delayed gamma, cargo container, nuclear material detection, photonuclear data.

1. INTRODUCTION

1.1. A new threat

In the last 10 years, terrorism threat has become a major preoccupation in the developed countries. Among all the forms of this threat, the possibility for a terrorist group to import a weapon of mass destruction (WMD) or even a “dirty” bomb (association of conventional explosive and nuclear material to contaminate a large area) in the heart of a big city has to be taken into account. In this context, the need of new and improved means for the detection of the smuggling of nuclear material in huge shipping containers becomes important. A lot of works are under development through the world to develop non-destructive inspection techniques to detect special nuclear materials inside containers, especially neutron interrogation based techniques[1]. In parallel, our work and other studies[2,3] have shown that photon irradiation techniques could play an important role in this context. Indeed, high-energy photons allow a deep inspection of large containers by penetrating sophisticated shielding materials. Moreover, the forward peaked bremsstrahlung photons can provide the exact localization of the nuclear material.

[*] mehdi.gmar@cea.fr; phone: +33 1 69 083 945; fax: + 33 1 69 086 030; www-list.cea.fr

1.2. From nuclear waste package characterization to cargo inspection

Up to now we have gained a large experience in the field of nuclear waste package characterization by photon activation and we have demonstrated that presently the detection limit can be less than one gram of actinide per ton of package[4]. In principle, the technique developed in this field can be adapted to the inspection of large cargo containers. The main differences are certainly the duration of inspection (typically tens of seconds), the volume of the object to inspect (standard cargo size: 2.4 m × 2.4 m × 6 m or 12 m) and the mass of actinides to detect (a few hundreds grams or more). The inspection of the container has not to impede the traffic, so it has to be as short as possible, probably less than a few minutes per container (a common duration in the literature is one minute[5]). Therefore, the key issue is certainly the inspection time.

2. METHOD

2.1. Principle

The method uses high-energy photons to induce photofission on actinides hidden in the container. During the fission process, the actinide splits in two nuclei called fission fragments. A short time after (10^{-17}s), neutrons and gammas are emitted by the fission fragments (the term prompt is used for these particles) and the child nuclei are called fission products. These fission products (being radioactive) will follow a β-decay chain to reach the valley of stability. In this process, some neutrons and gammas are emitted by the fission products. The delay between the photofission and the emission ranges from milliseconds to a few minutes (for the majority of decaying nuclei), and the term of delayed particles is used. The detection of delayed neutrons is the common way to detect and to assay actinides inside a package. Indeed, the detection efficiency can be good as neutron detectors can be large and not expensive. Moreover the signal-to-noise ratio can be high, provided that the incident photon energy is below the threshold of the reaction (γ,p) on ^{18}O (natural isotope of oxygen). Despite its faint abundance, this reaction is the main source of active noise above 15.9 MeV. The detection of delayed gammas can improve the detection and assessment of actinides and we have been among the first to propose this technique[6] as reported in the reference 5. Later Norman et al[7,8] experimentally demonstrated that a global measurement of high-energy gammas above 3 MeV was a distinctive and reliable signature of fissile materials in the case of fission induced by neutrons. In the case of photofission, we expected the same conclusion and our first measurements on nuclear waste package confirmed this point. The number of delayed high energy gammas from photofission is expected to be, at least, by 10 times greater than the number of delayed neutrons. Moreover, the detection of high-energy gammas can overcome some important limitations due to matrix effects like the presence of light elements. A key issue is the lack of consistent data for photofission in order to assess the performance of the method. In this paper we present the work in progress at CEA to provide these data. We have to note separately that some works were also dedicated to trying to use the detection of the neutron prompt signal to detect fissile material[9,10]. A drawback is that the incident photon energy has to be under the threshold of the (γ,n) reactions, about 8 MeV, otherwise the background dramatically increases. At least, the detection of prompt gammas does not seem possible because they are totally masked by probing photons (incident gamma flash).

2.2. Photofission rate

Photofission can occur if the energy brought by the probing photons is above the photofission threshold E_s, i.e. about 6 MeV for most of actinides. Compared to fission, the photofission cross-section is rather small, with a maximum of a few hundreds millibarns and peaked at 14 – 15 MeV. This drawback might be compensated by using a high-flux of photons generated by a powerful electron accelerator. The photofission rate is given by

$$f = \frac{MN_A}{m_{mol}} \int_{E_s}^{E_{max}} \phi(E)\sigma_f(E)\mathrm{d}E \,, \qquad (1)$$

where M is the mass of actinide, m_{mol} is the molar mass of the actinide, N_A Avogadro's number, σ_f the photofission cross-section (cm^2), $\phi(E)$ the flux of photons (photon.cm^{-2}.s^{-1}.MeV^{-1}) reaching the sample. In our case (see below), the flux of photons is produced by a beam of electrons hitting a tungsten target. To underline effects of spatial distribution of the sample and attenuation in the matrix and in the sample, equation (1) can be written in the form

$$f = \alpha_f \, f_o M \,, \tag{2}$$

where f_o is the photofission rate per gram of actinide if the sample is supposed to be punctual, with α_f being the attenuation and geometry factor. Figure 1 gives the dependence of the photofission rate versus the energy of electrons.

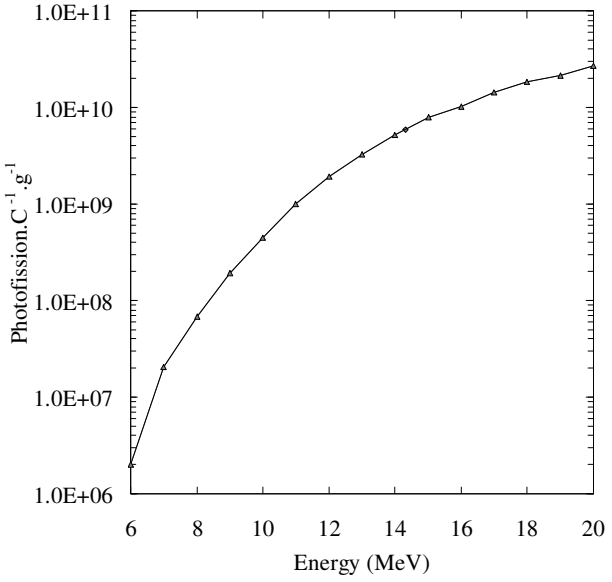

Figure 1: Photofission rate per coulomb and per gram of ^{238}U at 2 m
from a 5 mm-thick tungsten target versus the energy of incident electrons.

As shown by this figure the photofission rate increases with the energy of electrons. The choice of the energy will depend on the background noise and legal requirement concerning dose exposure of cargo containers. In the case of neutron activation, the neutron energy has to be under 10 MeV, the threshold of the reaction (n,p) on ^{16}O that produces a 6.13 MeV emitter with the 7.13 s half life[5]. This kind of limitation does not seem exist by using photons.

2.3. Delayed neutrons detection

Even if there are more than 270 known precursors of delayed neutrons that can be created by photofission, it is possible to gather precursors in six groups[11], each group being characterized by a half-life time and relative abundance yield. This method was proposed in the reactor physics for practical reasons. The mean number of neutrons emitted per fission depends on the actinide species. Temporal evolution of delayed neutrons can be described as a sum of six exponentials. If the detection of delayed neutrons is carried out between pulses, after l pulses, the number N_n of detected neutrons is given by

$$N_n = \varepsilon_n f \nu_d \sum_{i=1}^{6} \beta_i \Psi_i(l) \tag{3}$$

with

$$\Psi_i(l) = \frac{1}{\lambda_i}\left(1-e^{-\lambda_i t_p}\right)e^{-\lambda_i t_d}\left(1-e^{-\lambda_i t_c}\right)\frac{(l+1)(1-\omega_i)-(1-\omega_i^{l+1})}{(1-\omega_i)^2} \quad \text{and} \quad \omega_i = e^{-\lambda_i \tau},$$

where ε_n is the neutron detection efficiency, β_i therelative abundance yield of the group i, ν_d total number of delayed neutrons emitted per fission, $\ln(2)/\lambda_i$ half-life time of group i (s), t_p pulse duration (s), t_d time before starting counting (s), t_c counting time between two pulses (s), l total number of pulse, τ period of pulses, f photofission rate during pulse in the sample (photofission.s^{-1}). There are only a few experimental measurements of these parameters[12]. Recently, we have re-measured these ones in the case of ^{238}U. Our preliminary results seem to exhibit a good agreement with previous values

apart from the sixth group (the shortest half-life), as shown in table 1. Note that this difference is very important when short irradiation periods are used.

Groups	$\ln(2)/\lambda_i^{(a)}$	$\ln(2)/\lambda_i^{(b)}$	$\beta_i^{(a)}$	$\beta_i^{(b)}$
1	55.6 s	56.2 ± 0.8 s	1.7 ± 0.2	1.98 ± 0.08
2	21.88 ± 0.66 s	21.3 ± 0.3 s	16.5 ± 0.5	15.7 ± 0.5
3	5.01 ± 0.49 s	5.50 ± 0.20 s	18.3 ± 0.7	17.5 ± 0.7
4	2.07 ± 0.14 s	2.15 ± 0.10 s	37.3 ± 0.8	31.1 ± 0.8
5	0.584 ± 0.051 s	0.70 ± 0.06 s	18.0 ± 0.4	17.7 ± 0.9
6	0.174 ± 0.019 s	0.19 ± 0.02 s	8.5 ± 0.8	16.1 – 5, + 2

(a) Our measurements[14]
(b) Ref. 12

Table 1: Half-lives and relative abundance yields of the six groups of delayed neutrons from photofission of ^{238}U

2.4. Delayed gammas detection

Fission products emit not only delayed neutrons, but also delayed gammas. After an irradiation, all the materials surrounding the nuclear materials are activated, but a study of the gamma decay radiation data shows that very few activation products can emit gammas with energies above 3 MeV; indeed the majority of this signal can be attributed to the fission products. That is why the gamma measurement above 3 MeV provides a powerful method for actinides detection. As shown by the figure 2, a spectrum of delayed gammas emitted by a ^{238}U sample after an irradiation is very complex. This spectrum was obtained after an irradiation of 5.73 g of ^{238}U during 900 s and a cooling time of 10 s. The data accumulation time was 1800 s in this case. A pneumatic rabbit allowed the transfer of the sample in front of a HPGe diode in the interval of a few tenths of second after the irradiation.

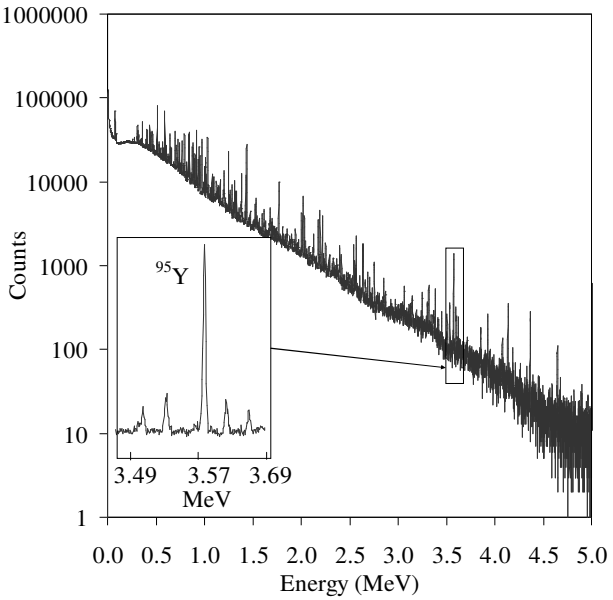

Figure 2: Photofission delayed gammas spectrum after an irradiation of 5.73 g of ^{238}U during 900 s and a cooling time of 10 s. The counting time is 1800 s.

Identification (according to half-life and gamma energy) and peak surface measurement brings the information on the corresponding fission product yield. We are currently working on this data analysis. Unfortunately, in order to assess the total emission yield above 3 MeV, identification of fission products by their main peak is not sufficient. Indeed, some of them emit numerous gammas above 3 MeV but generally with extremely weak intensity. For instance, ^{87}Br has more

than 200 gamma lines above 3 MeV and the strongest one has intensity of only 5.3 %. If we sum all the intensities above 3 MeV we obtain a rate of 0.68 gamma per disintegration. As the number of fission products is very large and their experimental yields are poorly known, it is difficult to calculate a realistic spectrum above 3 MeV. To overcome this problem, we can divide the spectrum in large energy bin and, in each energy group, analyze the time decay as a sum of exponentials (similarity to the delayed neutrons represented by a sum of exponentials). In this context, if the detection of delayed gammas is carried out after *l* pulses, the number of detected gammas is given by,

$$N_\gamma = f \sum_{k=1}^{g} \varepsilon_\gamma^k \eta_d^k \sum_{j=1}^{h} \gamma_j^k \Gamma_j^k (l) \tag{4}$$

with

$$\Gamma_j^k (l) = \frac{1}{\lambda_j^k} \left(1 - e^{-\lambda_j^k t_p}\right) e^{-\lambda_j^k T_d} \left(1 - e^{-\lambda_j^k T_c}\right) \left(\frac{1 - e^{-l \lambda_j^k \tau}}{1 - e^{-\lambda_j^k \tau}} \right)$$

where ε_γ^k is the gamma detection efficiency for energy bin *k*, γ_j^k the relative abundance yield of time group *j* and energy group *k*, η_d^k total number of delayed gammas emitted per photofission in the energy group *k*, ln(2)/ λ_j^k half-life group *j* and energy group *k* (s), t_p pulse duration (s), T_d time before starting counting (s), T_c counting time (s), *l* total number of pulses, τ period of pulses, *f* photofission rate during pulse in the sample (photofission.s^{-1}). To our knowledge, there are no parameters available on λ_j^k and η_d^k for photofission. Therefore, in parallel we launched two independent studies, one to measure individual fission product yields (in order to differenciate actinides inside nuclear waste package) and another one to make a global measurement of delayed gamma emitted by photofission, to detect the presence of actinides and to assay them inside nuclear waste packages and cargo containers. In fact, these studies are a part of a more general goal: the development of a new photonuclear activation file (PAF), which by now includes photonuclear cross sections for more than 600 isotopes including photofission fragment distributions and delayed neutrons tables for majority of actinides[14].

3. EXPERIMENTAL RESULTS

3.1. Experimental set-up

3.1.1. Photon sources: linear accelerators

All the measurements where carried out in two CEA's facilities called SAPHIR and ELSA[15]. Each facility houses a LINAC and with the benefit of their versatile characteristics, we are able to irradiate various objects from small samples to real size waste packages. SAPHIR is dedicated to the development of a method of characterization of nuclear waste packages by photon activation. The accelerator provides a pulsed electron beam at a frequency from 6.25 Hz to 400 Hz, each pulse lasting 2.5 µs with a maximum peak current of 100 mA. The energy ranges from 15 MeV to 30 MeV and can be changed in step of 5 MeV. To produce high-energy photons, the electrons hit a 5 mm-thick tungsten target cooled by light water. In this installation, even bulky objects (until 6 t) can be easily handled by the means of a dedicated conveyor. In addition, a pneumatic rabbit allows us to carry samples from the irradiation room to the front of various detectors. Another electron facility ELSA covers an energy range from 2 to 18 MeV with energy resolution lower than 100 keV for the high energies. ELSA can provide one or several micropulses of few picoseconds at a frequency ranging up to 72 kHz. The number of micropulses in one macropulse is limited to 10000 (140 µs). The maximum repetition rate of macropulses is 10 Hz. For safety reasons, the mean current is limited to 1 µA. The electrons hit a 1.2 mm-thick tantalum target with angle of 45° with respect to the beam direction. A collimator narrows the photon beam to reduce the background. By these characteristics ELSA is well adapted to the measurement of fundamental parameters.

3.1.2. Detection system

To detect the delayed signals we use commercially available components. Neutron detector block is made of three helium-3 counters embedded in a block of polyethylene wrapped with a cadmium foil. High-energy gammas are detected with a 127 mm-diameter and 76.2 mm-height BGO scintillator (127S76/5 BGO + pre-amplifier AS16, SAINT-GOBAIN).

3.2. Relative abundance yields and half-life groups measurement

In order to measure the relative abundance yields and half-life groups for photofission decay photons, an experimental campaign was launched at ELSA to assess these parameters for uranium 238. Each measurement consists of a repetitive cycle of irradiation and counting. The duration of irradiation and counting is changed in order to maximize the contribution of different groups with their characteristic decay periods. Four different cycles have been tested (irradiation time / counting time): 70 µs / 30 s, 10 s / 50 s, 60 s / 300 s and 300 s / 300 s. Each gamma event is recorded with two parameters, elapsed time since the end of the irradiation and energy. Figure 3 shows the time spectra of delayed high energy gammas. We believe that by fitting this experimental curve we will be able to get the different parameters of equation 4. Data processing of this experiment is under way.

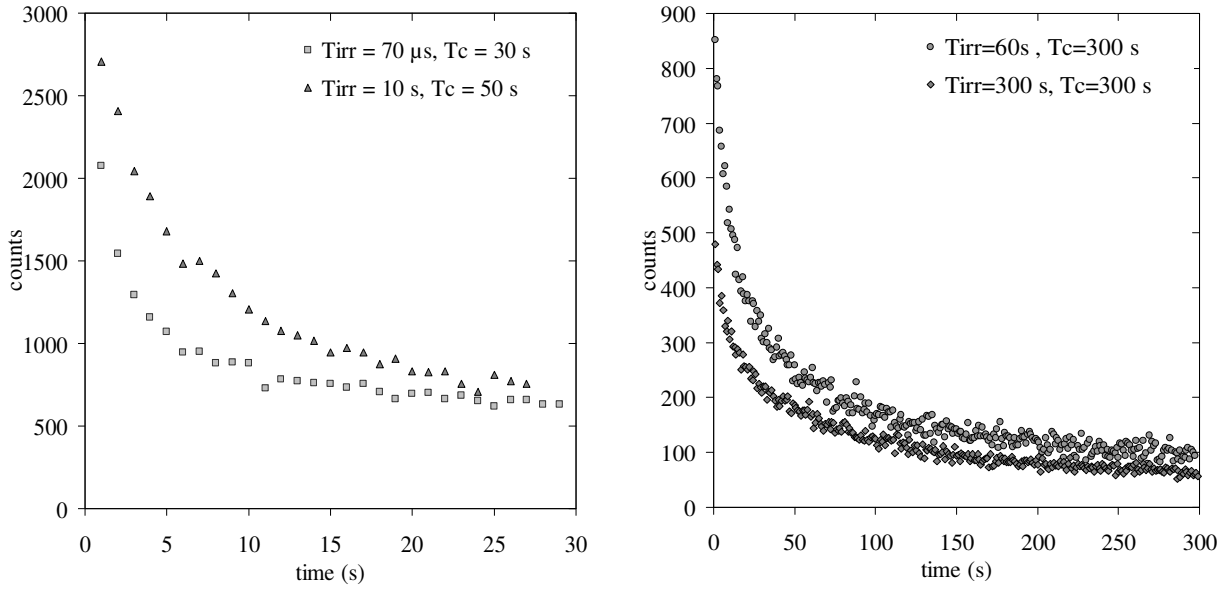

Figure 3: Raw decay gamma signal above 3 MeV for various time of irradiation and counting: photofission of ^{238}U.

At SAPHIR, we carried out a campaign of irradiation of uranium 238 to assess the influence of the irradiation time and the counting time on the number of delayed gamma detected in order to optimize these two parameters (see Figure 4). Equally, these data analysis is also still in progress.

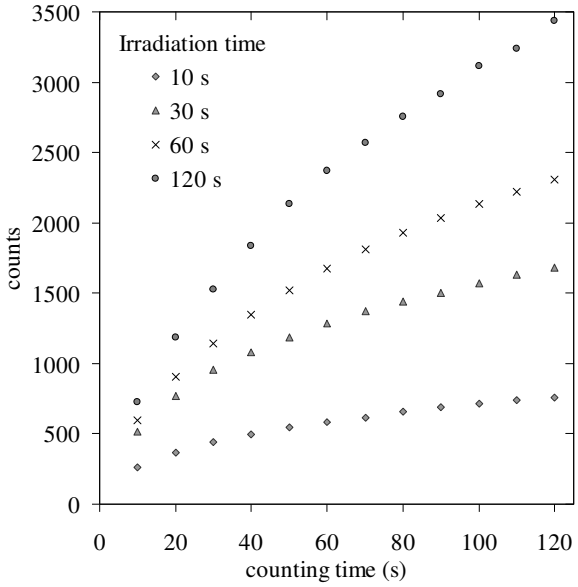

Figure 4: Number of decay gamma counts in the range 3 – 5 MeV versus the counting time for different irradiation times: photofission of ^{238}U.

3.3. First assessments on a mock-up container at SAPHIR

A mock-up of a container has been made to carry out measurements and assess the performances of the above described method. The container is a cube of 4.096 m^3. It is placed on a conveyor to be positioned in front of the photons flux (see Figure 5).

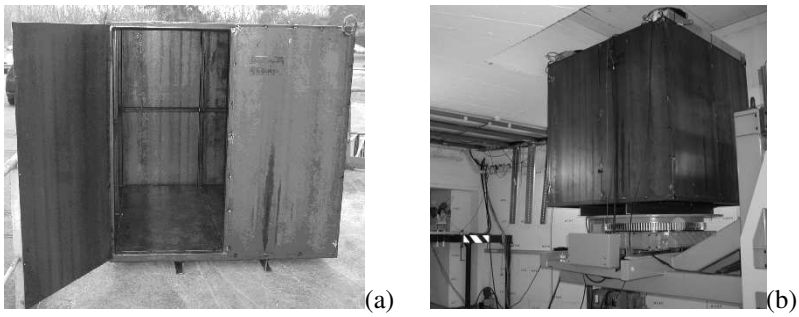

Figure 5: Photos of the mock-up of a container: a) container with opened doors, b) container in the irradiation position in the experimental hall.

For these first measurements, we used only two blocks of neutron detectors and a single BGO scintillator. The Figure 6 shows the acquisition chain, where we employed 3 (out 6) channels of the CANBERRA MULTIPORT II ADC. Two channels were dedicated for the neutrons detection in MCS mode and one for the gammas detection in PHA mode. The detectors were placed on the roof of the container (see Figure 7).

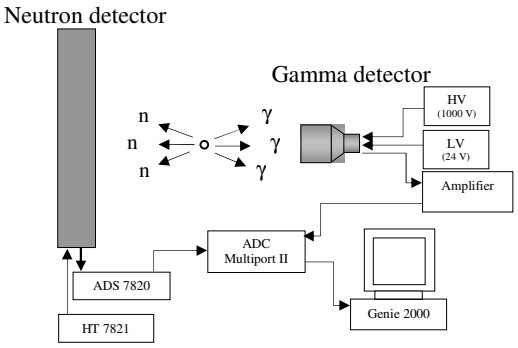

Figure 6: Acquisition chain of the experiment (see the text for details).

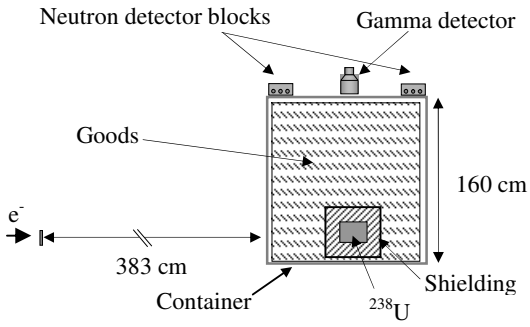

Figure 7: Scheme of the experimental set-up with the mock-up container.

Figure 8 shows the two decay photon spectra obtained during this experiment: active background (without actinide target present) and with a mass of 1.39 kg of uranium 238 placed in the empty container. The irradiation-decay cycle was 60 s - 60 s, correspondingly. The sample was placed at the container's bottom (see Figure 7). It is clearly seen from this simple experiment that the presence of the fissile material is a container can be observed without ambiguities. In the active background spectrum, the few counts above 3 MeV are probably due to a pile-up effect in the scintillator. We expect that the improvement of the electronic chain could increase further the signal-to-noise ratio.

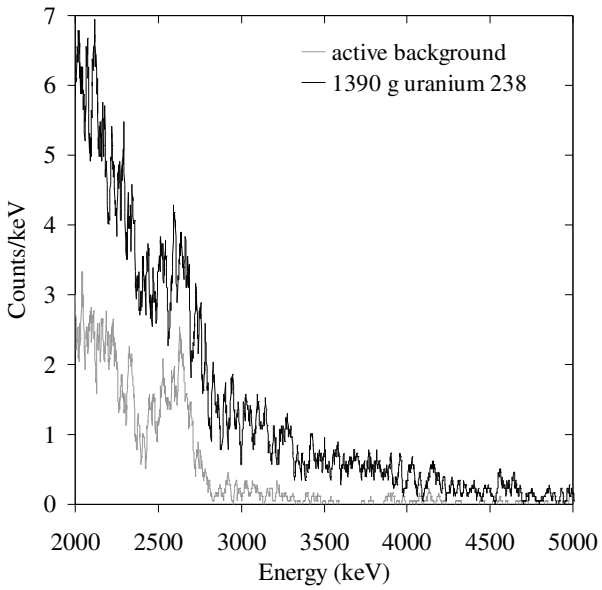

Figure 8: Decay photon energy spectra obtained with a ^{238}U sample of 1.39 kg and without (no actinide) in an empty container after an irradiation of 60 s and a counting of 60 s.

The experimental configuration allows us to test different shieldings and matrices. To illustrate the effects of the shielding on the intensity of delayed neutrons and delayed gammas, the same uranium sample was surrounded with high and low-Z materials. For each configuration, we measured the attenuation factor as the ratio between the detected counts in gamma and neutron with and without shielding (the active background subtracted). Figure 9 shows the result of these measurements.

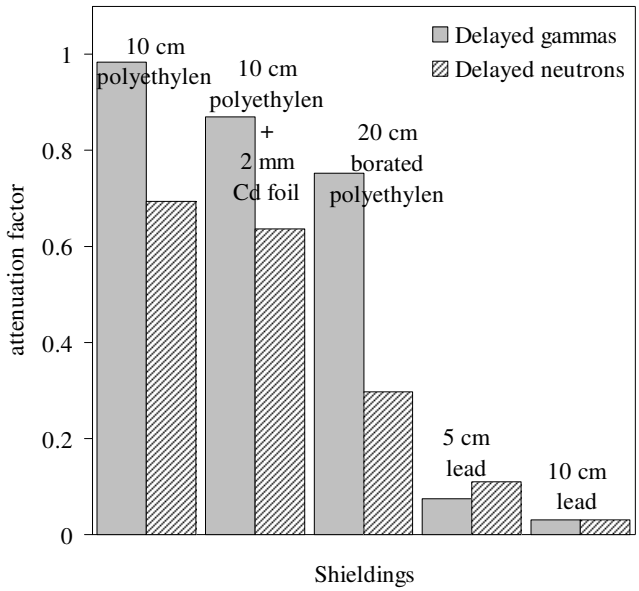

Figure 9: The measured attenuation factors for different shielding materials (see the legend and text for details).

As expected, the measurement of delayed gammas can overcome limitations due to the attenuation of delayed neutrons by light elements. An interesting point is that, in the case of a lead shielding (within our experimental configuration), the attenuation factor is roughly the same for neutrons and gammas. These two points show that the measurement of delayed gamma provides a more robust signature. In this configuration, the gamma net signal is 824 counts with just one gamma detector.

3.4. Delayed gammas over delayed neutrons ratio

During our experiments, we were be able to demonstrate that, in the case of uranium samples with different enrichment rates, the measurement of delayed gammas to delayed neutrons ratio can bring information on the isotopic composition of the sample. Indeed, if we suppose that there are q species of actinides inside the container and we consider a single photon energy bin, equations (3) and (4) can be written

$$N_\gamma = \varepsilon_\gamma \sum_{p=1}^{q} \left(\alpha_{\mathrm{f},p} f_{\mathrm{o},p} \eta_{\mathrm{d}}^{p} \sum_{j=1}^{h} \gamma_j^p \Gamma_j^p (l) \right) M_p \tag{5}$$

and

$$N_{\mathrm{n}} = \varepsilon_{\mathrm{n}} \sum_{p=1}^{q} \left(\alpha_{\mathrm{f},p} f_{\mathrm{o},p} \nu_{\mathrm{d}}^{p} \sum_{i=1}^{6} \beta_i^p \Psi_i^p (l) \right) M_p \ . \tag{6}$$

If we introduce the isotopic composition I_p and calculate the ratio R as the number of detected delayed gammas divided by the number of detected delayed neutrons, R is given by

$$R = \frac{N_\gamma}{N_{\mathrm{n}}} = \frac{\varepsilon_\gamma}{\varepsilon_{\mathrm{n}}} \frac{\sum_{p=1}^{q} \left(\alpha_{\mathrm{f},p} f_{\mathrm{o},p} \sum_{j=1}^{h} \gamma_j^p \eta_{\mathrm{d}}^p \Gamma_j^p (m) \right) I_p}{\sum_{p=1}^{q} \left(\alpha_{\mathrm{f},p} f_{\mathrm{o},p} \sum_{i=1}^{6} \beta_i^p \nu_{\mathrm{d}}^p \Psi_i^p (m) \right) I_p} = \frac{\varepsilon_\gamma}{\varepsilon_{\mathrm{n}}} \frac{\sum_{p=1}^{q} \varphi_p I_p}{\sum_{p=1}^{q} \xi_p I_p} \tag{7}$$

with

$$I_p = \frac{M_p}{\sum_{p=1}^{q} M_p} \ .$$

In the case of uranium 235 and uranium 238, we write

$$R = \frac{N_\gamma}{N_n} = \frac{\varepsilon_\gamma}{\varepsilon_n} \frac{\varphi_5 I_5 + \varphi_8 I_8}{\xi_5 I_5 + \xi_8 I_8} = \frac{\varepsilon_\gamma}{\varepsilon_n} \frac{(\varphi_5 - \varphi_8) I_5 + \varphi_8}{(\xi_5 - \xi_8) I_5 + \xi_8} \quad . \tag{8}$$

We irradiated several samples of uranium with different enrichment rates (from 0.7 % to 85 %) and we measured the delayed gammas to delayed neutrons ratio. Figure 10 shows this particular ratio measured with both the BGO and a HPGe detector. For delayed neutrons the same He-3 counters were used in both cases.

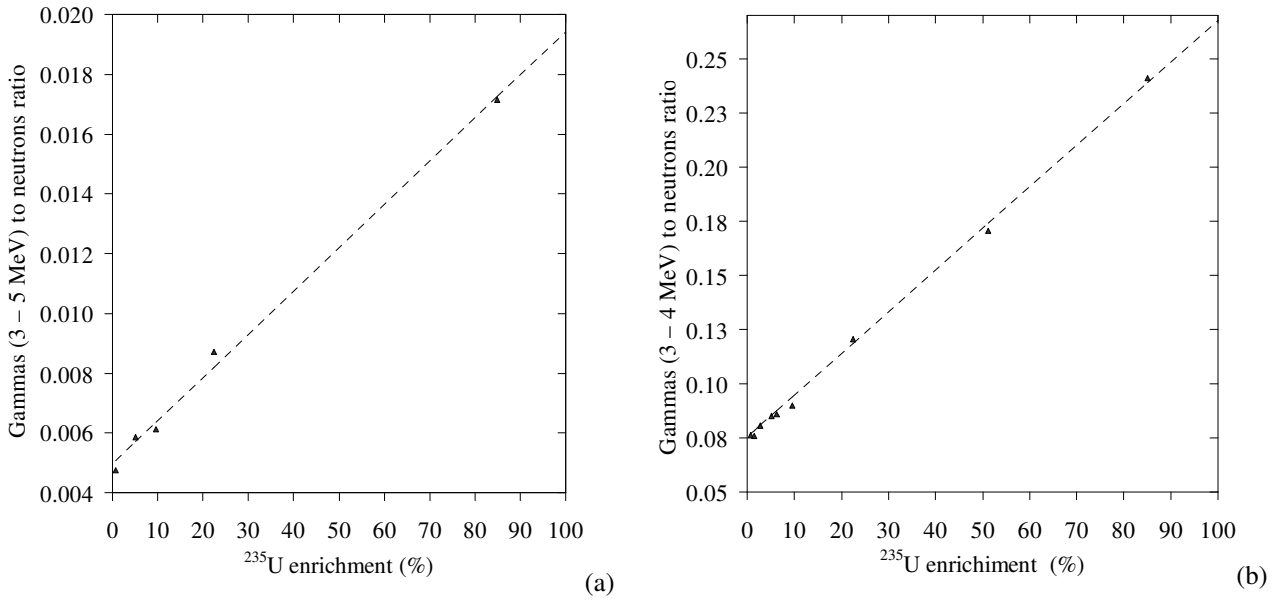

Figure 10: Delayed gammas over delayed neutrons ratio as a function of the ^{235}U enrichment (%)
(a) BGO detector, photon energy range: 3 – 5 MeV; (b) HPGe detector, photon energy range: 3 – 4 MeV

It clearly appears that the ratio *R* can give information on the isotopic composition in the case or uranium samples, provided that we are able to assess the ratio of gammas and neutrons efficiencies. Further data analysis along these lines is still in progress.

4. CONCLUSION

In this paper we have shown that an important effort is in progress at CEA to acquire basic photofission parameters both for delayed neutrons and delayed photons. Our first results using these particular observables to assess the performance of the photon interrogation method to inspect real size cargo containers are very encouraging. It seems that, the measurement of the photofission delayed neutrons and photons permits to inspect large objects as cargo containers in a short time and allows to overcome shielding effects. In addition, correlation of these two signals, in some cases, might provide an isotopic identification of nuclear materials.

ACKNOWLEDGMENT

We thank Xavier Ledoux of CEA/DIF for his helpful participation and advice during the experiments at ELSA.

REFERENCES

1. T. Gozani, "The role of neutron based inspection techniques in the post 9/11/01", *Nuc. Instr. and Meth. B*, **213**, 460 – 463, 2004.
2. J.L. Jones, W.Y. Yoon, D.R. Norman, K.J. Haskell, J.M. Zabriskie, S.M. Watson, J.W. Sterbentz, "Photonuclear-based, nuclear material detection system for cargo containers", *Nuc. Instr. and Meth. B*, **241**, 770 – 776, 2005.
3. D.R. Norman, J.L. Jones, W.Y. Yoon, K.J. Haskell, J.W. Sterbentz, J.M. Zabriskie, A.W. Hunt, F. Harmon, M.T. Kinlaw, "Inspection applications with higher electron beam energies", *Nuc. Instr. and Meth. B*, **241**, 787 – 792, 2005.
4. M. Gmar, F. Jeanneau, F. Lainé, H. Makil, B. Poumarède and F. Tola, "Assessment of actinide mass embedded in large concrete waste packages by photon interrogation and photofission", *Appl. Rad. and Isot.*, **63**, 613 – 619, 2005.
5. D.R. Slaughter, M.R. Accatino, A. Bernstein, J.A. Church, M.A. Descalle, T.B. Gosnell, J.M. Hall, A. Loshak, D.R. Manatt, G.J. Mauger, T.L. Moore, E.B. Norman, B.A. Pohl, J.A. Pruet, D.C. Petersen, R.S. Walling, D.L. Weirup, S.G. Prussin, M. McDowell, "Preliminary results utilizing high-energy fission product gamma-rays to detect fissionable material in cargo", UCRL-ID-155315, 2003.
6. M. Gmar and J. M. Capdevila, "Use of delayed gamma spectra for detection of actinides (U, Pu) by photofission", *Nuc. Instr. and Meth. B*, **422**, 841 – 845, 1999.
7. E.B. Norman, S. G. Prussin, R.-M. Larimer, H. Shugart, E. Browne, A.R. Smith, R. J. McDonald, H. Nitsche, P. Gupta, M.I. Frank, T.B. Gosnell, "Signatures of special nuclear material: High-energy γ-rays following fission", UCRL-JC-153259, 2003.
8. E.B. Norman, S.G. Prussin, R.-M Larimera, H. Shugart, E. Browne, A.R. Smitha, R.J. McDonald, H. Nitsche, P. Gupta, M.I. Frank, T.B. Gosnell, "Signatures of fissile materials: high-energy γ rays following fission", *Nuc. Instr. and Meth. A*, **521**, 608 – 610, 2004.
9. B.J. Micklich, D.L. Smith, "Nuclear materials detection using high-energy gamma-rays", *Nuc. Instr. and Meth. B*, **241**, 782 – 786, 2005.
10. B.J. Micklich, D.L. Smith, T.N. Massey, C.L. Fink, D. Ingram, "FIGARO: detecting nuclear materials using high-energy gamma-rays", *Nuc. Instr. and Meth. A*, **505**, 466 – 469, 2003.
11. R.W Waldo, R.A Karam, R.A. Meyer, *Phys. Rev. C*, **23**, 1113 – 1127, 1981.
12. O.P. Nikotin, K. A. Petrzhak, "Delayed neutrons in the photofission of heavy nuclei", Soviet Atomic Energy, 20, 300 – 303, 1966.
13. D. Doré, J.C. David, M.L. Giacri, J. M. Laborie, X. Ledoux, D. Ridikas, A. Van Lauwe, "Delayed neutron yields and spectra from photofission of actinides with Bremsstrahlung photons below 20 MeV", *Proc. of the 19th Nuclear Physics Divisional Conf. on New Trends in Nuclear Physics Application and Technology (NPDC19)*, Pavia (Italy), 2005.
14. D. Ridikas, M.-L. Giacri, M.B. Chadwick, J.-C. David, D. Doré, X. Ledoux, A. Van Lauwe and W.B. Wilson, "Status of the photonuclear activation file: Reaction cross-sections, fission fragments and delayed neutrons", *Nuc. Instr. and Meth. A*, accepted for publication, 2006.
15. P. Guimbal et al., "Status of the ELSA-2 project", *EPAC'02 proceedings*, Paris (France), 2002.